Qualitative and quantitative characterisation of adsorption mechanisms of lead on four biochars

Journal:	*Environmental Science & Technology*
Manuscript ID	es-2016-054174
Manuscript Type:	Article
Date Submitted by the Author:	26-Oct-2016
Complete List of Authors:	Shen, Zhengtao; Geotechnical and Environmental Research Group, Department of Engineering Zhang, Yiyun; University of Cambridge, Department of Engineering Jin, Fei; University of Cambridge, Department of Engineering McMillan, Oliver; University of Cambridge, Department of Engineering Al-Tabbaa, Abir; University of Cambridge, Department of Engineering

Environmental Science & Technology

WSP700 (Wheat straw pellets biochar produced at 700 °C)

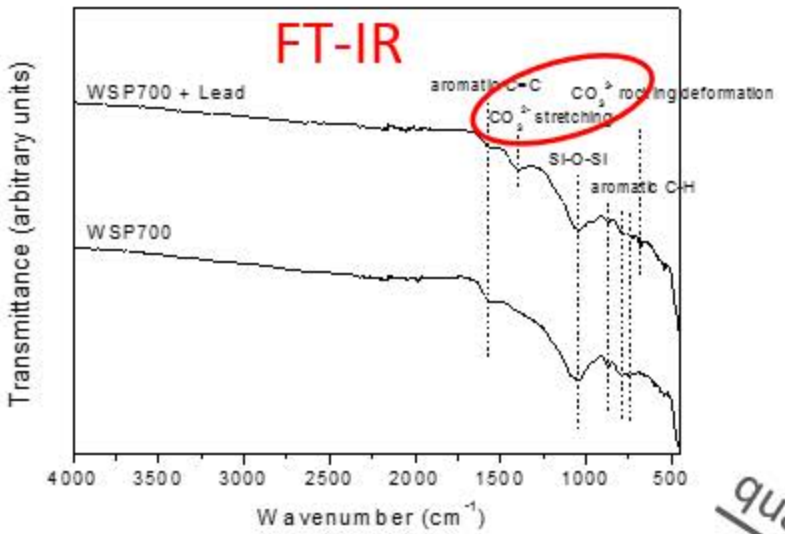

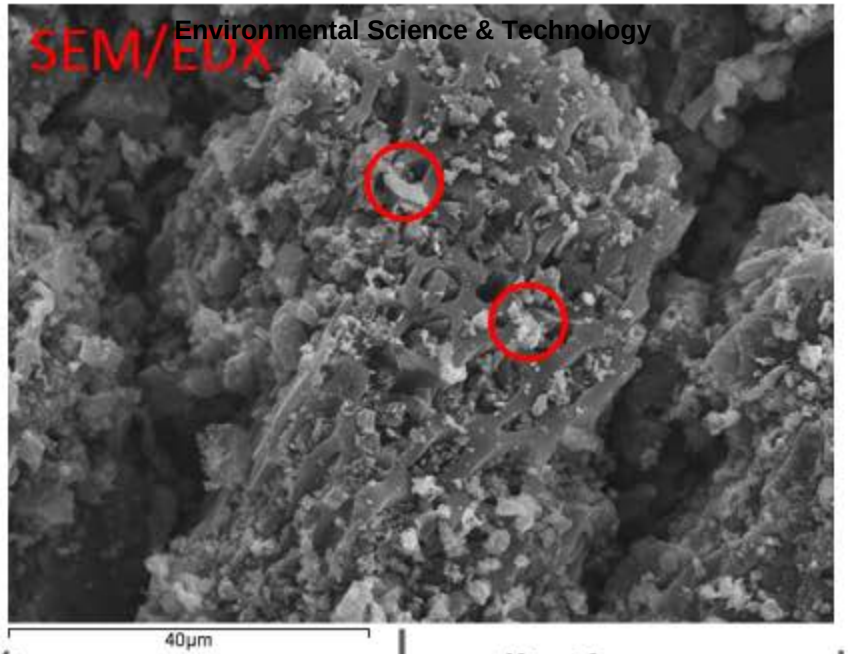

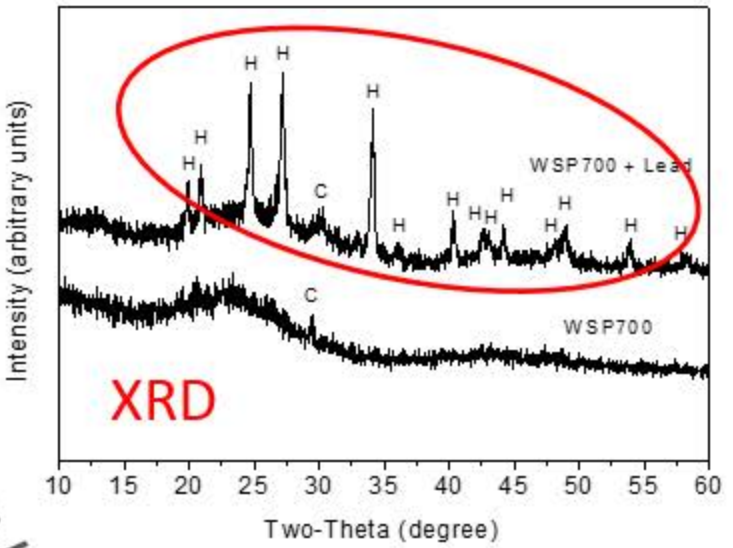

qualitative

qualitative

qualitative

Hydrocerussite

$(Pb_3(CO_3)_2(OH)_2)$

quantitative

quantitative

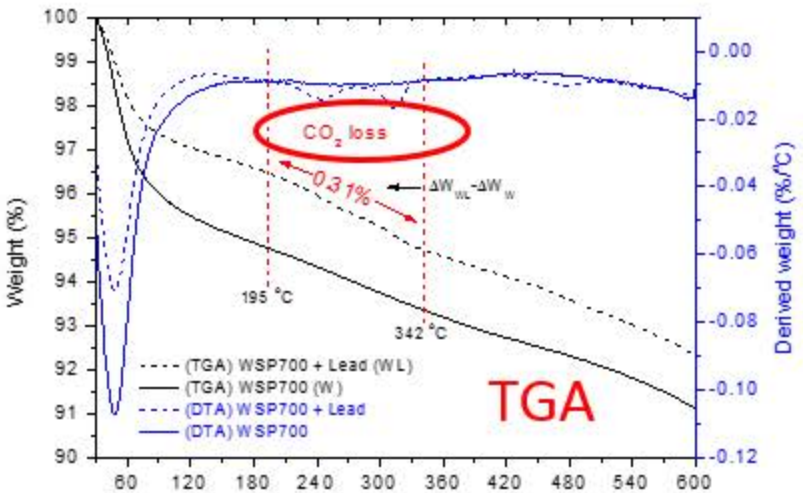

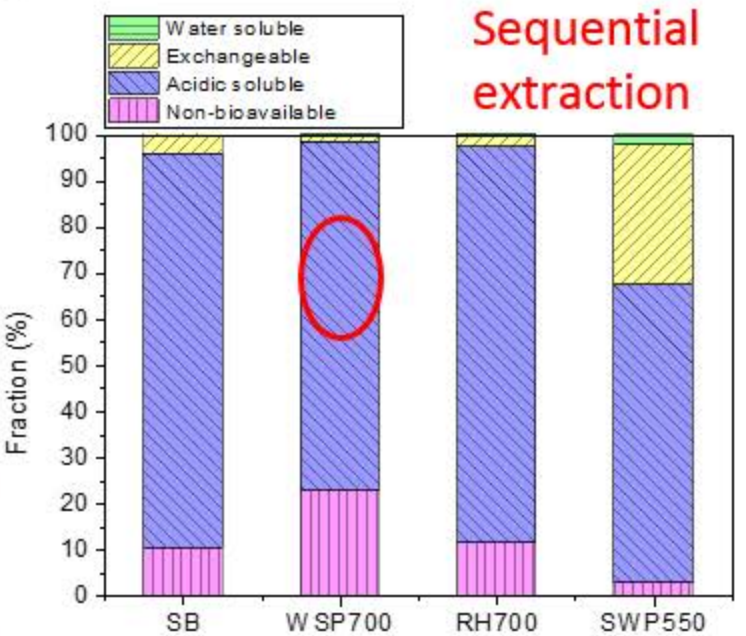

Characterise the adsorption mechanisms of Pb^{2+} on biochars

Qualitative and quantitative characterisation of adsorption mechanisms of lead on four biochars

Zhengtao Shen,*[,1] Yiyun Zhang,[1] Fei Jin,[1] Oliver McMillan,[1] and Abir Al-Tabbaa[1]

[1](Geotechnical and Environmental Research Group, Department of Engineering, University of Cambridge, Cambridge, CB2 1PZ, United Kingdom)

*Corresponding author: Email: ztshennju@gmail.com; zs281@cam.ac.uk. Phone number: 0044+7541935253. Fax: 0044+7541935253

Abstract: The adsorption mechanisms of lead (Pb^{2+}) on four biochars (SB produced from British hardwood at 600 ℃ and three standard biochars produced from wheat straw pellets at 700 ℃ (WSP700), rice husk at 700 ℃ (RH700) and soft wood pellets at 550 ℃ (SWP550)) were characterised qualitatively and quantitatively, using a combination of chemical and micro-structural methods. Sequential extraction test results show that Pb^{2+} was predominantly adsorbed on SB (85.31%), WSP700 (75.61%) and RH700 (85.76%) as acidic soluble fraction, which was potentially bioavailable if applied in soil. Micro-structural analysis further investigated this fraction and confirmed the presence of cerussite ($PbCO_3$) on SB and hydrocerussite ($Pb_3(CO_3)_2(OH)_2$) on WSP700, RH 700 and SWP550, suggesting a mechanism of surface precipitation for Pb^{2+} adsorption on the biochars. The percentages of $PbCO_3$ on SB (82.24%) and $Pb_3(CO_3)_2(OH)_2$ on WSP700 (13.00%), RH 700 (19.19%) and SWP550 (29.70%) were quantified using thermogravimetric analysis (TGA). This study suggests that it is feasible to quantify different adsorption mechanisms of Pb^{2+} on biochars, which is important for the practical application of biochar in water and/or soil treatment.

Keywords: biochar, quantitative, characterisation, adsorption mechanism, lead, speciation

1 Introduction

Biochar is a charcoal-like material produced from agricultural and industrial organic wastes to store carbon[1,2]. Pyrolysis is the typical production process for biochar during which the feedstock (typically biomass) is carbonised and subsequently biochar, bio-oil and syn-gas are produced[2,3]. The engineered biochar was proposed to have high adsorption capacities for heavy metals due to its high pH, surface area and cation exchange capacity (CEC) as well as active aromatic structure[1,2,4]. Applying biochar in water treatment or soil remediation to adsorb or immobilise heavy metals and consequently reduce their environmental risks was regarded as a green sustainable remediation technology considering its additional benefits in waste management, energy production and carbon storage[5].

Adsorption is the main mechanism for biochar to treat heavy metals in water and soil[6]. Biochar can adsorb heavy metals through a range of mechanisms including physical adsorption, cation exchange, cation-π interaction, surface precipitation and surface complexation[7–11]. Different adsorption mechanisms have different environmental implications. The adsorbed heavy metals on biochar through physical adsorption and cation exchange represent readily bioavailable fraction in soil which poses direct risks to plants and humans, whereas those through cation-π interaction represent potentially bioavailable fraction and those through surface complexation represent non-bioavailable fraction[12]. The bioavailability of heavy metals adsorbed on biochar through surface precipitation depends on precipitate type: the formed precipitates that can be dissolved in sodium acetate/acetic acid is regarded as potentially bioavailable and the rest is regarded as non-bioavailable. When applied to contaminated soil, it is expected that biochar could reduce the readily bioavailable heavy metals to reduce the environmental risks. However, when applied in water treatment, the physically bonded and exchangeable heavy metals on biochar are easier to be desorbed, which will aid the reuse of biochar. The adsorption mechanisms of heavy metals on biochar vary among biochars produced from different feedstocks at different temperatures due to their different properties[8-11]. Therefore it is important to identify the adsorption mechanisms of heavy metals on biochar in order to direct its practical applications and predict its environmental performances. In addition, when applied to field contaminated land, the environmental factors such as rainfall, groundwater flow, soil microbial activity, plant

and earthworm may affect the long-term effectiveness of the immobilisation of heavy metals by biochar. Understanding the adsorption mechanisms of heavy metals on biochar prior to field application will aid the selection of biochar, the engineering design and estimation/modelling of the resistance and long-term stability of biochar immobilisation of heavy metals on field conditions.

Batch adsorption studies are the most conventional methods to investigate the adsorption mechanisms of heavy metals on biochar. The adsorption mechanisms could be inferred through the adsorption characteristics obtained from batch adsorption studies. Micro-structural methods such as X-ray diffraction (XRD), Fourier transformed infrared (FT-IR) spectra and scanning electron microscopy (SEM) and energy dispersive X-ray (EDX) analysis are typically used accompanying with batch adsorption studies to indicate the adsorption mechanisms of heavy metals on biochar[13–15]. The formed minerals, the change of the molecular structure and the surface morphology of biochar after heavy metal adsorption can be identified as to indicate the adsorption mechanisms. However, these micro-structural analyses remain at a qualitative level to date, very limited investigations focusing on quantifying the portions of heavy metals adsorbed on biochar through different mechanisms have been carried out. Xu et al. (2014)[16] quantified the portions of different precipitates on a manure and a rice straw biochar after Pb^{2+} adsorption using MINTEQ modelling (accompanied with adsorption studies, XRD and FT-IR tests). They found 91.6% and 67.5% of adsorbed Pb^{2+} on the inorganic part of the two biochars can be attributed to precipitation, and subsequently quantified the portions of different precipitates ($Pb_5(PO_4)_3Cl$ and $Pb_3(CO_3)_2(OH)_2$). However, experimental results are needed to verify these findings obtained through MINTEQ modelling. Fristak et al.[17] used a chemical method called sequential extraction combined with adsorption studies and FT-IR analysis to investigate the adsorption mechanisms both qualitatively and quantitatively. They found 69-92% of Cd^{2+} was adsorbed on two woody biochars and an activated carbon as exchangeable and acidic soluble fractions, whereas 61.8-72.4% of Cu^{2+} was adsorbed through complexation. However this study did not quantitatively separate the exchangeable and acidic soluble fractions of heavy metals on biochars which pose different environmental risks. The quantification of the adsorption mechanisms of heavy metals on biochar needs further understanding.

It is therefore important to characterise the adsorption mechanisms of heavy metals on biochar both qualitatively and quantitatively to aid its practical application. In this study, XRD, FT-IR and SEM/EDX were used to qualitatively investigate the sorption mechanisms of lead (Pb^{2+}) on biochars. A modified sequential extraction test was used to quantify different speciation of Pb^{2+} on biochar representing different environmental risks. Thermogravimetric analysis (TGA) was used to quantify the thermally decomposable minerals formed on biochar after heavy metal adsorption. This experimental study aims to investigate the adsorption mechanisms of Pb^{2+} on biochar both qualitatively and quantitatively, so as to aid the understanding of its environmental implications.

2 Materials and methods

2.1 Biochar

Four biochars were used in this study. Salisbury biochar (SB) was obtained from Southern Woodland Products (Salisbury, UK). It was produced from British broadleaf hardwood at a pyrolysis temperature of 600 ºC in a retort with a residence time of 13.5 h. SB was previously applied to a field contaminated site in the UK and exhibited excellent performance in immobilising Ni^{2+} and Zn^{2+} in sandy soil in a three-year study[18]. In contrast, SB did not affect the mobility or speciation of Pb^{2+} in kaolin in a short-term study[19]. Therefore SB was chosen in this study to further investigate its adsorption mechanisms for heavy metals. In previous studies, the adsorption characteristics of heavy metals on eight biochars, produced and recommended by the UK Biochar Research Centre (UKBRC) at the University of Edinburgh as standard biochars, were investigated[20,21]. Wheat straw pellets biochar produced at 700 ℃ (WSP700), rice husk biochar produced at 700 ℃ (RH700), and soft wood pellets biochar produced at 550 ℃ (SWP550) were selected to be studied in this study as they exhibited the highest, moderate and the lowest adsorption capacities for heavy metals among the eight standard biochars. The biochars were oven dried at 60 ℃ for 48 h and ground and sieved to a particle size smaller than 0.15 mm. The selected physicochemical properties of SB, WSP700, RH700 and SWP550 can be found from the previous studies and are also shown in Table 1.

Table 1 Selected physicochemical properties of biochars[18-21].

	SB	WSP700	RH700	SWP550
BET surface area (m^2/g)	5.30	23.20	42.00	26.40
Cation exchange capacity (cmol/kg)	7.20	12.50	5.36	2.53
pH	6.96	10.03	9.81	7.91
pH_{pzc}	6.3	7.4	7.5	7.8
Volatile matter (%)	N.A.	7.38	4.99	14.20
Total ash (%)	N.A.	23.82	47.93	1.25
C (%)	79.91	69.04	47.32	85.52
H (%)	N.A.	1.18	0.63	2.77
O (%)	N.A.	5.30	2.06	10.36
N (%)	0.73	1.32	0.85	<0.10
P (%)	N.A.	0.25	0.16	0.06
Pb (%)	0.01	bdl	bdl	bdl

(N.A. – not available, bdl – below detection limit)

2.2 Chemical and micro-structural analyses

Pb^{2+} was selected as the target metal in this study as it is among the most serious concerns for water and soil pollution[22] and all the four biochars exhibited the highest adsorption capacities for Pb^{2+} compared with other heavy metals[20,21,23]. A measured amount of biochar (0.1 g) was added to 20 mL solution of 5 mM $Pb(NO_3)_2$ (pH=5) containing 0.01 M $NaNO_3$. The mixture was shaken at 200 rpm for 24 h to reach adsorption equilibrium and then centrifuged at 4000 rpm for 3 minutes (same centrifugation condition hereafter). The liquid was discarded and the biochar was quickly washed using 20 mL deionised water and the water was discarded after centrifugation. A pre-trial study indicates that the influence of washing on the total amount of adsorbed Pb^{2+} was negligible. The remained solid was oven dried at 60 ℃ for 48 h to represent the biochar sample after Pb^{2+} adsorption for chemical and micro-structural analysis. The same procedure above was employed on the control sample without the presence of $Pb(NO_3)_2$ to represent the biochar sample before Pb^{2+} adsorption for FT-IR, XRD and TGA tests. In order to qualitatively and quantitatively characterise the adsorption mechanisms, the biochar samples before and after Pb^{2+} adsorption were examined using the following chemical and micro-structural analyses.

The 5-step sequential extraction test was typically used to indicate the speciation and bioavailability of heavy metals in soil[24–26]. As sequential extraction is a time consuming test method, it is useful if the test method could be simplified while being kept efficient in determining the heavy metal speciation. Since steps 3, 4 and 5 in the conventional method represent non-bioavailable fractions of heavy metals, a simplified 4-step sequential extraction was developed in which the original steps 3, 4 and 5 were combined. In addition, a step representing the water soluble or physically adsorbed fraction of heavy metals on biochar was added to determine their readily bioavailable fraction in soil. The two steps representing exchangeable (readily bioavailable) and acidic soluble (potentially bioavailable) fractions respectively in the 5-step procedure remained in the 4-step procedure. The Pb^{2+} in the solid residue from the equilibrium study (as detailed above) was extracted and defined as the following four steps:

Step 1 – water soluble fraction: The solid residue (0.1 g biochar + adsorbed Pb^{2+}) was mixed with 20 mL deionised water and shaken for 24 h at room temperature (20 ℃);

Step 2 – exchangeable fraction: The residue from step 1 was extracted with 8 mL of 0.5 M $MgCl_2$ (adjusted to pH 7.0 using NaOH or HCl) and shaken for 20min at room temperature;

Step 3 – acidic soluble fraction: The residue from Step 2 was extracted with 8 mL of 1 M NaOAc (adjusted to pH 5.0 with HOAc) and shaken for 5 h at room temperature;

Step 4 – non-bioavailable fraction: The residue from step 3 was digested with 9 mL of 36% HCl and 3mL of 70% HNO_3 for 16 h at room temperature and then heated at 95 ℃ for 2 h.

In sequential extraction, shaking in step 1, 2 and 3 was performed at 200 rpm. Following each step, the samples were centrifuged at room temperature. The supernatant was then collected and filtered through a 0.45 μm filter and acidified or diluted when necessary before analysis with inductively coupled plasma/optical emission spectrometry (ICP-OES) (Perkin-Elmer, 7000DV) to determine the Pb^{2+} concentration. The remaining solid sample was washed with 20 mL deionised water prior to the next extraction step, and the washing solution was discarded after centrifugation.

XRD was used to indicate the crystalline phases in the sample. The dry samples were mounted on a flat holder and examined by a Siemens D500 X-ray diffractometer with a CuKα source operating at 40 kV and 40 mA, emitting radiation at a wavelength of 1.5405 Angstroms. The scanning regions were between 10-60° of 2θ values at a rate of 0.6 s/step and a resolution of 0.02°/step.

FT-IR was used to study the fundamental vibrations and associated rotational-vibrational structure. The infrared spectrum of biochar was tested by a Perkin Elmer Spectrum 100 Fourier transform infrared spectroscopy spectrometer. 16 scans were taken from 4000 to 450 cm^{-1} with a resolution of 4 cm^{-1}.

TGA measures the weight loss with precision while heating the biochar samples. In order to quantify the possible precipitates (e.g. cerussite and hydrocerussite) that formed after biochar adsorption of Pb^{2+}, the biochar sample was analysed using Mettler-Toledo TGA/DSC 1 Thermogravimetric Analyzer. Approximately 10 mg biochar samples were placed into the ceramic crucible and heated from 30 to 600 ℃ at a heating rate of 10 ℃/min under N_2 atmosphere at flow rate of 30 mL/min. The first derivatives of the TG curves (DTG) were calculated to identify the thermal decomposition of the possible precipitates.

SB was coated with gold and its surface morphology was examined by a Phenom Pro desktop Scanning electron microscopy at 5 kV. The surface morphology of the WSP700, RH700 and SWP550 were examined by a FEI Quanta 200 FEI system with an acceleration voltage of 20 kV after being coated with gold. After Pb^{2+} adsorption, the surface morphology and elemental composition of biochars were examined by a JSM-5800LV SEM with EDX at 10 kV after being coated with Pd.

2.3 Quality control

Sequential extraction test was performed in duplicates. All micro-structural tests were carried out once, with pre-trials being conducted to check the reproducibility. The preparation of biochar samples and sequential extraction test were conducted at a temperature controlled lab at 20 ± 1 ℃ and 50 ± 2% humidity. The micro-structural tests were carried out at ambient temperatures.

3 Results and discussion

3.1 Sequential extraction results

The speciation of Pb^{2+} determined by sequential extraction test is shown in Figure 1. The recovery of the sequential extraction test is shown in Table S1. The recovery of Pb^{2+} from SB, WSP700 and RH700 was 78.41-85.52%, while that for SWP550 (46.16%) was much lower. The sequential extraction recovery of Pb^{2+} from SB, WSP700 and RH700 is similar to the recovery of heavy metals from biochar or biochar treated soils using conventional sequential extraction methods in previous studies. Fristak et al.[17] conducted a 4-step sequential extraction test (steps 2, 3, 4 and 5 in conventional methods) on two woody biochars after adsorption of Cd^{2+}, Zn^{2+} and Cu^{2+}, and observed a recovery range of 82.4-104.4%. The conventional sequential extraction recovery of Pb^{2+} from SB treated soil was 61.50-97.28%[19]. SWP550, which has the lowest recovery, also reveals the lowest adsorption capacity of Pb^{2+}, indicating that sequential extraction tests may not work well for samples with low adsorbed heavy metal contents due to the large relative standard errors. The discussion about the sequential extraction results below will not include SWP550 considering its low recovery.

The sequential extraction results indicate that the majority of adsorbed Pb^{2+} on SB (85.31%), WSP700 (75.61%) and RH700 (85.76%) fall in acidic soluble fraction. WSP700 has 22.86% non-bioavailable fraction whereas this fraction for SB and RH700 was 10.4% and 11.4% respectively. The exchangeable fraction for all the three biochars was low (1.38-4.29%) and their water soluble fraction was negligible (0-0.14%). The negligible water soluble fraction suggests the adsorption of Pb^{2+} to the three biochars was a chemical rather than physical process[27]. The low exchangeable fraction together with the negligible water soluble fraction indicates an absence of readily bioavailable fraction of Pb^{2+} on the three biochars. The majority of Pb^{2+} was acidic soluble which represents a potentially bioavailable fraction. This fraction may come from the formation of Pb^{2+} precipitates which can be dissolved in the NaOAc/HOAc solution (step 3 in sequential extraction). Alternatively, it may result from the adsorbed Pb^{2+} on biochar through cation-π interaction. Table S2 shows the change of solution pH between step 2 and 3. It can be found that the equilibrium solution pH decreased from above pH_{pzc} to below pH_{pzc} which would result in the change of biochar surface charge from negative to positive, therefore the adsorbed Pb^{2+} through cation-π interaction can be desorbed at step 3 due to electrostatic repulsion[9,28]. The non-bioavailable fraction may come from the

adsorbed Pb^{2+} from surface complexation or the formation of precipitates that cannot be dissolved in the NaOAc/HOAc solution.

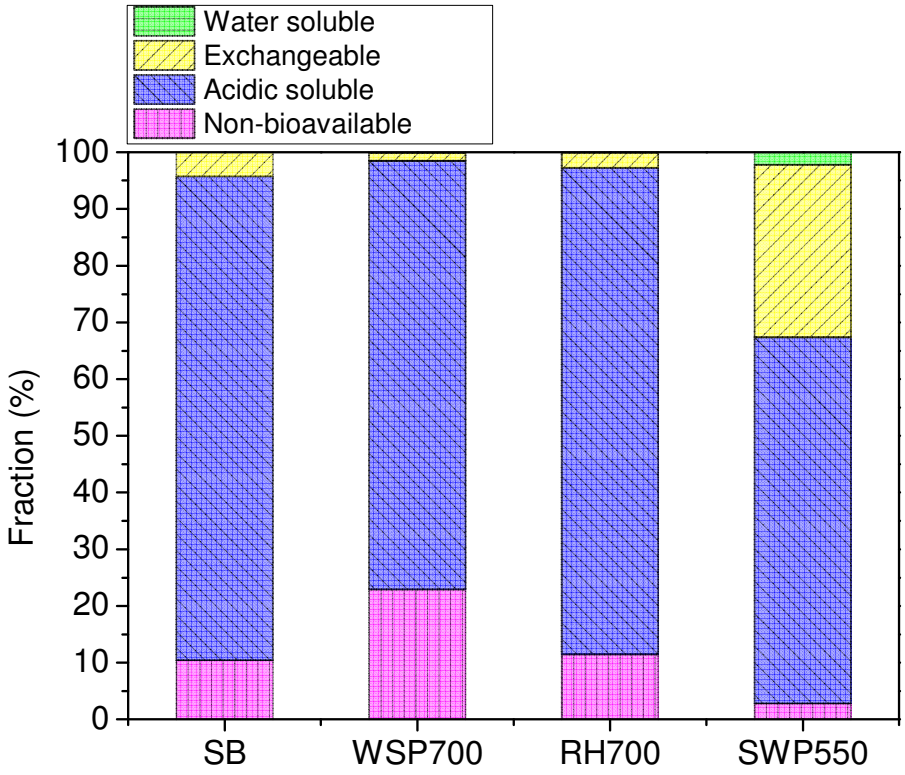

Figure 1 Speciation of lead on biochars.

3.2 XRD and FT-IR results

It was found from the sequential extraction results that the majority of Pb^{2+} on SB, WSP700 and RH700 falls in acidic soluble fraction, representing an adsorption mechanism of either surface precipitation or cation-π interaction. XRD and FT-IR tests were applied to biochar samples to verify the formation of precipitates and changes of functional groups caused by cation-π interaction respectively.

The XRD patterns of the four biochars are shown in Figure 2. Strong evidence was obtained from XRD patterns suggesting the formation of cerussite ($PbCO_3$) on SB, and hydrocerussite ($Pb_3(CO_3)_2(OH)_2$) on WSP700, RH 700 and SWP550. The CO_3^{2-} that formed these precipitates could be generated from the carbonates in biochar formed during production due to the decomposition of carboxylates[30], which is supported by the presence of calcite ($CaCO_3$) in SB and WSP700 suggested by XRD patterns (Figure 2a and 2b). The absence of peaks associated with carbonates

for RH700 and SWP550 (Figure 2c and 2d) may be due to that their concentrations were below the limit of detection (LOD). The CO_3^{2-} may also come from the dissolved CO_2 in solution from the air during adsorption tests. It can be found that a higher biochar pH (WSP700, RH 700 and SWP550) favoured the formation of $Pb_3(CO_3)_2(OH)_2$ while a lower biochar pH (SB) aided the formation of $PbCO_3$ in this study.

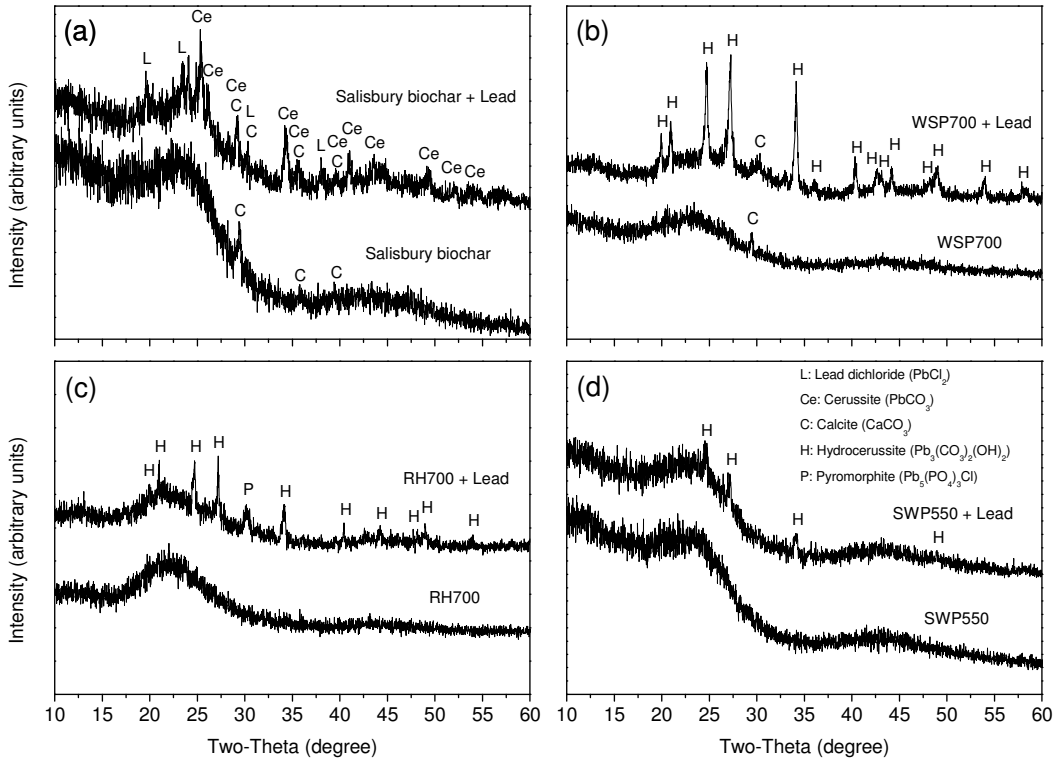

Figure 2 XRD patterns of biochars before and after Pb^{2+} adsorption (a – Salisbury biochar (SB), b – WSP700, c – RH700, d – SWP550).

The FT-IR spectra of the four biochars are shown in Figure 3. A new peak representing CO_3^{2-} stretching was observed on FT-IR spectra of WSP700 after Pb^{2+} adsorption (Figure 3a), which was very likely from the $Pb_3(CO_3)_2(OH)_2$ as suggested by the XRD results. The minerals formed on SB, RH700 or SWP550 suggested by XRD patterns were not identified by FT-IR test, probably due to their lower contents (below LOD). The peaks associated with aromatic C for the four biochars did not reveal significant changes after Pb^{2+} adsorption. Shifts of FT-IR peaks associated with functional groups such as carbonyl, hydroxyl and ester were observed for water hyacinths biochars after Cd^{2+} and Pb^{2+} adsorption in a previous study[31], suggesting

an adsorption mechanism of electrostatic interaction between biochars and heavy metals. However, the present study did not find evidence from FT-IR suggesting an adsorption mechanism of electrostatic interaction or cation-π interaction, which may be due to the detection limit.

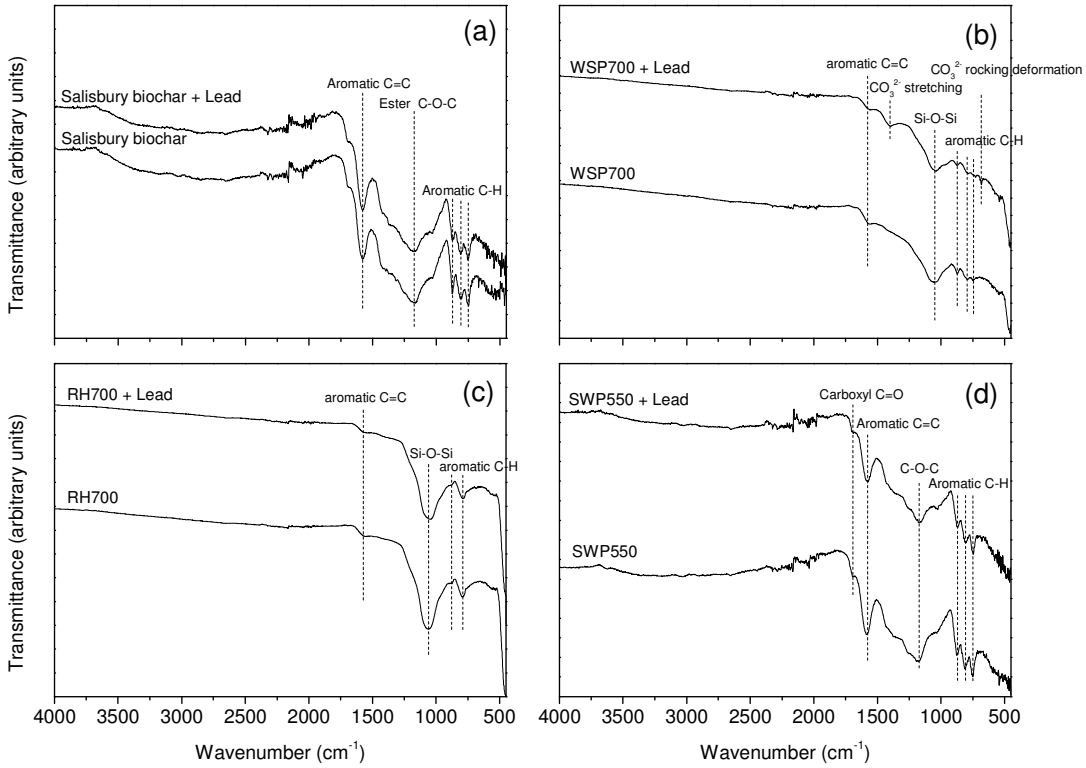

Figure 3 FT-IR spectra of biochars before and after Pb^{2+} adsorption (a – Salisbury biochar (SB), b – WSP700, c – RH700, d – SWP550).

3.3 TGA results

TGA tests were carried out to find out the contents of $Pb_3(CO_3)_2(OH)_2$ or $PbCO_3$ on biochars and the results are shown in Figure 4. $CaCO_3$, lead dichloride ($PbCl_2$) and pyromorphite ($Pb_5(PO_4)_3Cl$) that suggested by XRD results on biochars are stable at the testing temperature range[32,33]. Two new peaks on DTG curve between 223 and 361 ℃ for SB after Pb^{2+} adsorption (Figure 4a) were attributed to the thermal decomposition of $PbCO_3$[34], further confirming a sorption mechanism of surface precipitation. It is of note that various intermediate products (e.g. $PbCO_3 \cdot PbO$ and $PbCO_3 \cdot 2PbO$) may form during the thermal decomposition of $PbCO_3$ to PbO[35], which can be affected by the experimental conditions and the influence of other substances

in the biochar. The two peaks indicate the presence of such intermediate products. However, regardless of the type of the intermediate products, the weight loss between 223 and 361 ℃ was all referred to CO_2 loss. The decomposition of $PbCO_3$ to PbO (if only considering the final products) can be expressed as:

$$PbCO_3 \rightarrow PbO + CO_2 \qquad \text{Equation 1}$$

According to the TGA results and Equation 1 and taking the biochar sample before Pb^{2+} adsorption as a control, the weight percentage of Pb^{2+} in the form of $PbCO_3$ can be calculated as 3.11%, which is equivalent to 82.24% of the totally adsorbed amount of Pb^{2+} on SB. It was calculated from the sequential extraction results that 85.31% of the totally adsorbed Pb^{2+} on SB was acidic soluble, which coincides well with the TGA results and suggests this acidic soluble fraction was mainly in the form of $PbCO_3$.

Similar to $PbCO_3$, the thermal decomposition of $Pb_3(CO_3)_2(OH)_2$ at the testing temperature range can be separated to several steps. The dehydration process ($Pb_3(CO_3)_2(OH)_2$ to $2PbCO_3{\cdot}PbO$) took place within 100-200 ℃[36], and then the decomposition of $2PbCO_3{\cdot}PbO$ to PbO happened between 260-370℃ during which a range of intermediate products may present (e.g. $PbCO_3{\cdot}PbO$, $4PbCO_3{\cdot}3PbO$ and $PbCO_3{\cdot}2PbO$)[34]. In this study, the dehydration of $Pb_3(CO_3)_2(OH)_2$ overlapped with the drying process of biochar, which was therefore difficult to be isolated (the big peaks on DTG curves before ~200 ℃ in Figure 4). However this will not affect the calculation of the percentage of $Pb_3(CO_3)_2(OH)_2$ on biochar. The new peaks on DTG curves within 195-342 ℃, 286-339 ℃ and 288-375 ℃ for WSP700, RH700 and SWP550 after Pb^{2+} adsorption respectively indicate the presence of the intermediate products, further suggesting a sorption mechanism of surface precipitation. Regardless of the type of the intermediate products, the weight loss ($2PbCO_3{\cdot}PbO$ to PbO) was all referred to CO_2 loss, and therefore the percentage of Pb^{2+} in the form of $Pb_3(CO_3)_2(OH)_2$ on biochar can be calculated based on Equation 1.

According to the TGA results and Equation 1, the percentage of Pb^{2+} in the form of $Pb_3(CO_3)_2(OH)_2$ on WSP700, RH700 and SWP550 can be calculated as 1.46%, 0.66% and 0.24% (taking the biochar samples before heavy metal adsorption as control), which are equivalent to 13.00%, 19.19% and 29.70% of the totally adsorbed Pb^{2+}

respectively. The sequential extraction results show 75.61% and 85.76% of totally adsorbed Pb^{2+} are acidic soluble for WSP700 and RH700 respectively. Therefore, according to the TGA results, there are other mechanisms in addition to the formation of $Pb_3(CO_3)_2(OH)_2$ accounting for the acidic soluble fraction of Pb^{2+} on WSP700 and RH700, such as the formation of other acidic soluble minerals that were not detected by TGA tests or cation-π interaction between biochar and Pb^{2+}.

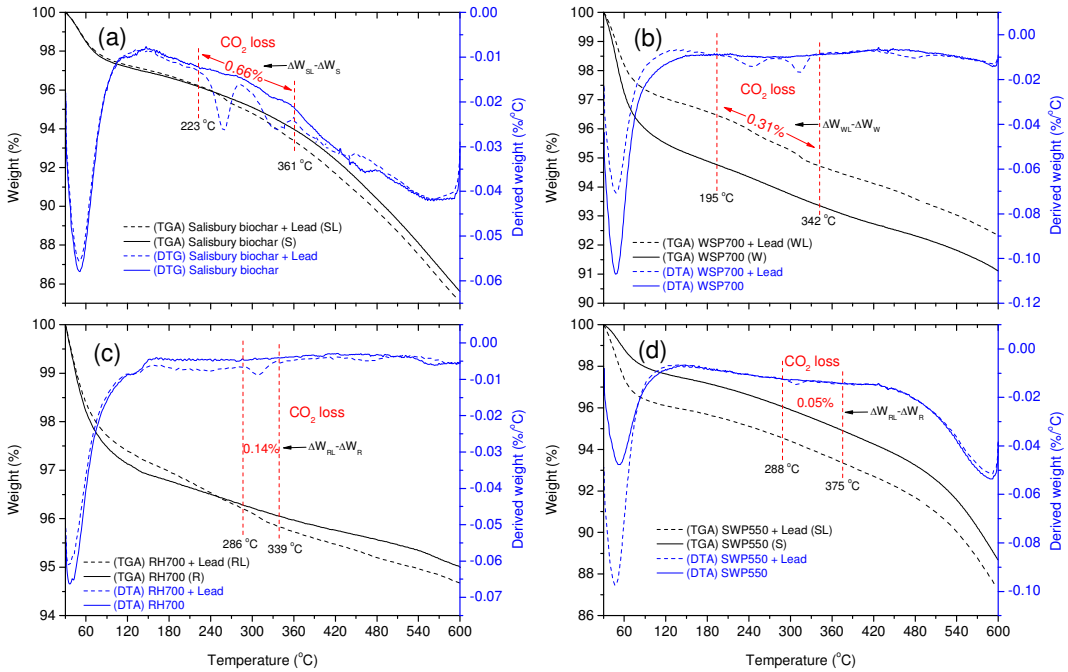

Figure 4 TGA and DTG curves of biochars before and after Pb^{2+} adsorption (a – Salisbury biochar (SB), b – WSP700, c – RH700, d – SWP550).

3.4 SEM and EDX results

The SEM images and EDX results of biochar were shown in Figure 5, Figure 6, S1, S2, S3, S4 and S5. Pb^{2+} was observed on the surface of SB (Figure 5 and S3). This Pb^{2+} may come from Pb^{2+} precipitates as suggested by XRD, FT-IR and TGA results. The presence of Al^{3+} also suggests it may have exchanged with Al^{3+} on biochar. EDX plots for WSP700 showed the presence of Pb^{2+} both perpendicular and parallel to fibre direction (Figure S4). Clear solid particles can be seen from plot 1, 3, 5 and 6 (Figure 6 and S4), suggesting the formation of Pb^{2+} precipitates as suggested by XRD and TGA results. Pb^{2+} was also observed on RH700 (Figure S2 and S5), which may either come from Pb^{2+} precipitates or through cation exchange with K^+ or Ca^{2+}.

The EDX results for SWP550 did not show Pb^{2+} (Figure S1), which was likely due to the relatively low contents of Pb^{2+} on SWP550.

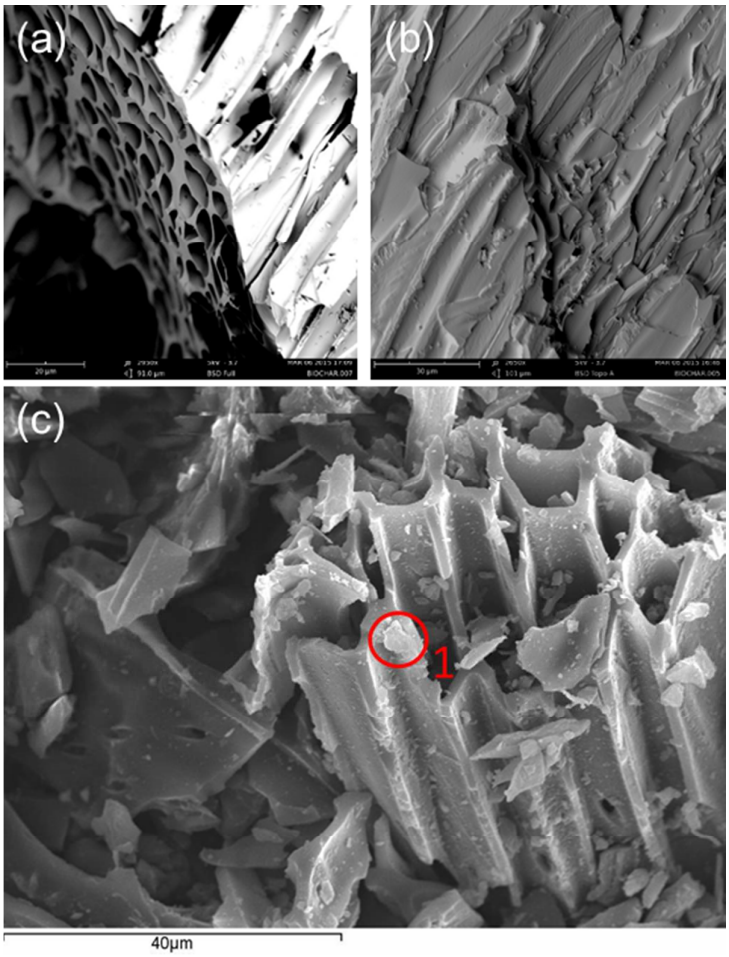

Figure 5 SEM/EDX images of SB before and after Pb^{2+} adsorption (a – perpendicular to fibre direction before adsorption[23], b – parallel to fibre direction before adsorption, c – perpendicular to fibre direction after adsorption, the spectrum for the EDX plot (red circle) was shown in Figure S3).

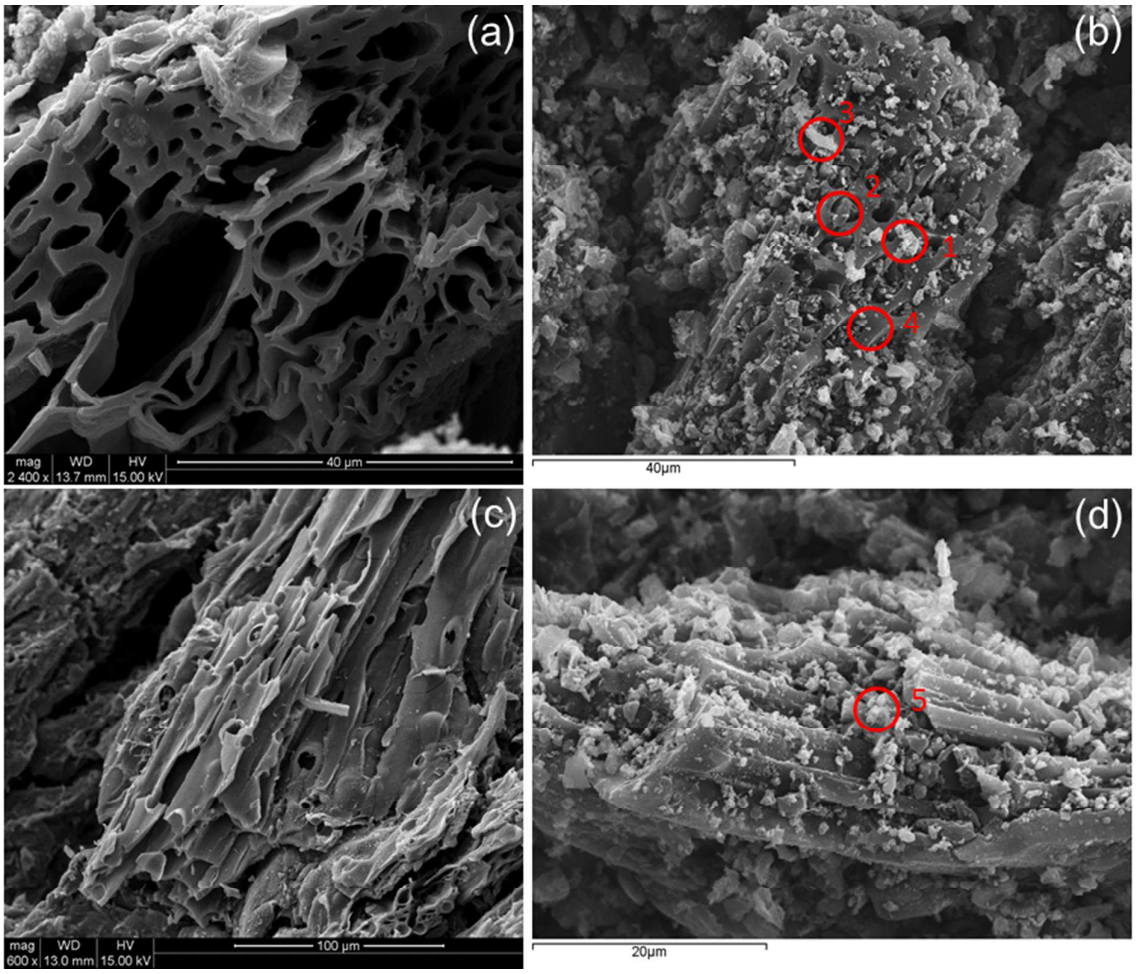

Figure 6 SEM/EDX images of WSP700 before and after Pb^{2+} adsorption (a – perpendicular to fibre direction before adsorption[21], b – perpendicular to fibre direction after adsorption, c – parallel to fibre direction before adsorption, d – parallel to fibre direction after adsorption, the spectrums for the EDX plots (red circles) were shown in Figure S4).

3.4 Environmental implications

SB was previously applied to a field contaminated site (sandy soil)[18] and an artificially contaminated clay soil (kaolin) in laboratory[19]. It effectively immobilised Ni^{2+}, Zn^{2+} and Pb^{2+} (data for Pb^{2+} not shown) in the field site through increasing their non-bioavailable (residual) fraction during a three-year study, while it did not show significant influence on the mobility or speciation of Pb^{2+} in the kaolin during a 28-day study. It was suggested that the insignificant effect was due to the failure for SB to competitively adsorb Pb^{2+} against kaolin in the acidic environment (pH 4.54-4.92)[19]. The present study coincides with that previous study and further confirms

that the main mechanism for Pb^{2+} adsorption on SB was through precipitation to $PbCO_3$ and therefore it was difficult for SB to precipitate Pb^{2+} and alter its speciation in the kaolin under such an acidic environment. However, according to the findings from the present study, considering the soil pH (7.9-8.1) of the field site soil[18], the immobilisation mechanism of Pb^{2+} would likely be the formation of acidic soluble precipitates on biochar surface representing a potentially bioavailable fraction in the site soil on field conditions, which conflicts with the findings that the addition of SB increased the non-bioavailable (residual) fraction of heavy metals (Ni^{2+}, Zn^{2+} and Pb^{2+}) on site[18]. Previous studies observed that biochar immobilised heavy metals (Cu^{2+}, Pb^{2+} or Cd^{2+}) to different fractions (e.g. acidic soluble fraction[37], reducible and oxidisable fractions[38] and residual fraction[39]) in soils. However these studies did not investigate the speciation of heavy metals after being adsorbed on biochar in aqueous solutions. Therefore the comparison between heavy metal speciation under the two environments (water and soil) cannot be made in those studies. Therefore no references can be found to give hints to the explanation of the conflicts findings in the immobilisation mechanism between this study and the site study[18]. It may be due to that the alkaline soil aid biochar's adsorption for heavy metals through precipitation to stable minerals; or biochar strengthened the bonding of heavy metals (residual fraction) to soils.

Previous studies found that pH and CEC can be good indicators for the adsorption capacities of heavy metals (Cu^{2+}, Ni^{2+} and Pb^{2+}) on the standard biochars, with higher pH and CEC resulting in higher adsorption capacities, which were attributed to the formation of alkaline minerals and an accompanied aromaticity during biochar production[20,21,30]. This study confirms a majority portion of acidic soluble Pb^{2+} on WSP700 and RH700, suggesting adsorption mechanisms of surface precipitation and/or cation-π interaction, which is in line with the previous analysis that alkaline minerals and/or accompanied aromaticity determined the adsorption of heavy metals on the standard biochars[20,21]. This study also observed that cation exchange made a very small contribution to the adsorption of Pb^{2+} on WSP700 and RH700, suggesting that cation exchange played an insignificant role in Pb^{2+} adsorption on the standard biochars and CEC was only an indicator of alkaline mineral contents.

This study quantified different speciation of Pb^{2+} on SB, WSP700 and RH700. The majority of Pb^{2+} were adsorbed on biochar as an acidic soluble fraction, which

represents potentially bioavailable fraction if applied in soil. Within the acidic soluble fraction, the percentage of adsorbed Pb^{2+} through precipitation to $PbCO_3$ on SB and $Pb_3(CO_3)_2(OH)_2$ on WSP700 and RH700 was quantified. Therefore the long-term stability of this fraction on field conditions can be estimated based on the solubility of these precipitates, the site conditions and local climate if these biochars were applied to field contaminated land. It is also possible to model the long-term performance of biochar for soil remediation if the adsorption mechanisms can be quantified and other environmental parameters can be obtained. The adsorption mechanisms contributing to other acidic soluble Pb^{2+} on the biochars (e.g. formation of other precipitates or cation-π interaction) were not identified due to the detection limits of XRD and FT-IR tests. Based on the evidence found from this study, the properties of biochar may be altered by controlling the production process so as to specify the most suitable biochars for a specific engineering usage, however the linkage between biochar field performance and laboratory test results needs careful verification before large-scale application.

Acknowledgement

Special thanks go to Dr. Kai Gu from Nanjing University, China, who kindly offered the TGA tests for this study. The standard biochars were obtained from the UK Biochar Research Centre (UKBRC) at the University of Edinburgh. The authors would like to thank Dr. Ondrej Masek from the UKBRC for his kind help in preparing and delivering the biochar samples. Special thanks also go to Dr. Zhen Li from the College of Resources and Environmental Sciences, Nanjing Agricultural University, China, who conducted the SEM tests for the biochars used in this study.

References

(1) Lehmann, J. Bio-energy in the black. *Front. Ecol. Environ.* **2007**, *5*, 381–387.

(2) Sohi, S. P. Carbon storage with benefits. *Science* **2012**, *338*, 1034–1035.

(3) Jahirul, M. I.; Rasul, M. G.; Chowdhury, A. A.; Ashwath, N. Biofuels production through biomass pyrolysis- A technological review. *Energies* **2012**, *5*, 4952–5001.

(4) Beesley, L.; Moreno-Jiménez, E.; Gomez-Eyles, J. L.; Harris, E.; Robinson, B.; Sizmur, T. A review of biochars' potential role in the remediation, revegetation and restoration of contaminated soils. *Environ. Pollut.* **2011**, *159*, 3269–3282.

(5) Lehmann, J.; Gaunt, J.; Rondon, M. Bio-char sequestration in terrestrial ecosystems - A review. *Mitig. Adapt. Strateg. Glob. Chang.* **2006**, *11*, 403–427.

(6) Sizmur, T.; Quilliam, R.; Puga, A. P.; Moreno-Jiménez, E.; Beesley, L.; Gomez-Eyles, J. L. Application of Biochar for Soil Remediation. In *Agricultural and Environmental Applications of Biochar: Advances and Barriers*; Guo, M., He, Z., Uchimiya, S. M., Eds; Soil Science Society of America, Inc **2016**; pp 295–324.

(7) Cao, X.; Ma, L.; Gao, B.; Harris, W. Dairy-manure derived biochar effectively sorbs lead and atrazine. *Environ. Sci. Technol.* **2009**, *43*, 3285–3291.

(8) Choy, K. K. H.; McKay, G. Sorption of cadmium, copper, and zinc ions onto bone char using Crank diffusion model. *Chemosphere* **2005**, *60*, 1141–1150.

(9) Keiluweit, M.; Nico, P. S.; Johnson, M.; Kleber, M. Dynamic molecular structure of plant biomass-derived black carbon (biochar). *Environ. Sci. Technol.* **2010**, *44*, 1247–1253.

(10) Mohan, D.; Pittman, C. U.; Bricka, M.; Smith, F.; Yancey, B.; Mohammad, J.; Steele, P. H.; Alexandre-Franco, M. F.; Gómez-Serrano, V.; Gong, H. Sorption of arsenic, cadmium, and lead by chars produced from fast pyrolysis of wood and bark during bio-oil production. *J. Colloid Interface Sci.* **2007**, *310*, 57–73.

(11) Zhang, Y.; Tang, X.; Luo, W. Metal Removal with Two Biochars Made from Municipal Organic Waste: Adsorptive Characterization and Surface Complexation Modeling. *Toxicol. Environ. Chem.* **2015**, *2248*, 1–30.

(12) Rodriguez-Vila, A.; Asensio, V.; Forjan, R.; Covelo, E. F. Chemical fractionation of Cu, Ni, Pb and Zn in a mine soil amended with compost and biochar and vegetated with Brassica juncea L. *J. Geochemical Explor.* **2015**, *158*, 74–81.

(13) Cui, X.; Fang, S.; Yao, Y.; Li, T.; Ni, Q.; Yang, X.; He, Z. Science of the Total Environment Potential mechanisms of cadmium removal from aqueous

solution by Canna indica derived biochar. *Sci. Total Environ.* **2016**, *562*, 517–525.

(14) Cheng, Q.; Huang, Q.; Khan, S.; Liu, Y.; Liao, Z.; Li, G.; Ok, Y. S. Adsorption of Cd by peanut husks and peanut husk biochar from aqueous solutions. *Ecol. Eng.* **2016**, *87*, 240–245.

(15) DeMessie, B.; Sahle-Demessie, E.; Sorial, G. A. Cleaning Water Contaminated With Heavy Metal Ions Using Pyrolyzed Biochar Adsorbents. *Sep. Sci. Technol.* **2015**, *50*, 2448–2457.

(16) Xu, X.; Cao, X.; Zhao, L.; Zhou, H.; Luo, Q. Interaction of organic and inorganic fractions of biochar with Pb (II) removal by biochar. *RSC Adv.* **2014**, *4*, 44930–44937.

(17) Fristak, V.; Pipiska, M.; Lesny, J.; Soja, G.; Friesl-Hanl, W.; Packova, a. Utilization of biochar sorbents for Cd(2)(+), Zn(2)(+), and Cu(2)(+) ions separation from aqueous solutions: comparative study. *Env. Monit Assess* **2015**, *187*, 4093.

(18) Shen, Z.; Som, A. M.; Wang, F.; Jin, F.; McMillan, O.; Al-Tabbaa, A. Long-term impact of biochar on the immobilisation of nickel (II) and zinc (II) and the revegetation of a contaminated site. *Sci. Total Environ.* **2016**, *542*, 771–776.

(19) Shen, Z.; McMillan, O.; Jin, F.; Al-Tabbaa, A. Salisbury biochar did not affect the mobility or speciation of lead in kaolin in a short-term laboratory study. *J. Hazard. Mater.* **2016**, *316*, 214–220.

(20) Shen, Z.; Zhang, Y.; Jin, F.; McMillan, O.; Al-Tabbaa, A. Characteristics and mechanism of nickel sorption on four standard biochars produced at 550 ℃ and 700 ℃. *J. Hazard. Mater.* **2016**, *under review*.

(21) Shen, Z.; Zhang, Y.; Jin, F.; McMillan, O.; Al-Tabbaa, A. Adsorption characteristics and mechanisms of nickel on soft wood pellets and mescanthus straw pellets biochars. **2016**, *in preparation*.

(22) Yang, Y.; Wei, Z.; Zhang, X.; Chen, X.; Yue, D.; Yin, Q.; Xiao, L.; Yang, L. Biochar from Alternanthera philoxeroides could remove Pb(II) efficiently. *Bioresour. Technol.* **2014**, *171*, 227–232.

(23) Shen, Z.; Jin, F.; Wang, F.; McMillan, O.; Al-Tabbaa, A. Sorption of lead by Salisbury biochar produced from British broadleaf hardwood. *Bioresour. Technol.* **2015**, *193*, 553–556.

(24) Tessier, A.; Campbell, P. G. C.; Bisson, M. Sequential extraction procedure for the speciation of particulate trace metals. *Anal. Chem.* **1979**, *51*, 844–851.

(25) Li, X.; Coles, B. J.; Ramsey, M. H.; Thornton, I. Sequential extraction of soils for multielement analysis by ICP-AES. *Chemical Geology* **1995**, *124*, 109–123.

(26) Li, X. D.; Poon, C. S.; Sun, H.; Lo, I. M.; Kirk, D. W. Heavy metal speciation and leaching behaviors in cement based solidified/stabilized waste materials. *J. Hazard. Mater.* **2001**, *82*, 215–230.

(27) Inyang, M. I.; Gao, B.; Yao, Y.; Xue, Y.; Zimmerman, A.; Mosa, A.; Pullammanappallil, P.; Ok, Y. S.; Cao, X. A Review of Biochar as a Low-Cost Adsorbent for Aqueous Heavy Metal Removal. *Crit. Rev. Environ. Sci. Technol.* **2016**, *46*, 406–433.

(28) Gao, H.; Sun, Y.; Zhou, J.; Xu, R.; Duan, H. Mussel-inspired synthesis of polydopamine-functionalized graphene hydrogel as reusable adsorbents for water purification. *ACS Appl. Mater. Interfaces* **2013**, *5*, 425–432.

(29) Shen, Z.; Jin, F.; Wang, F.; Mcmillan, O.; Al-tabbaa, A. Sorption of lead by Salisbury biochar produced from British broadleaf hardwood. *Bioresour. Technol.* **2015**, *193*, 553–556.

(30) Dodson, J. Wheat straw ash and its use as a silica source. Ph.D. Dissertation, University of York, **2011**.

(31) Ding, Y.; Liu, Y.; Liu, S.; Li, Z.; Tan, X.; Huang, X.; Zeng, G.; Zhou, Y.; Zheng, B.; Cai, X. Competitive removal of Cd(ii) and Pb(ii) by biochars produced from water hyacinths: performance and mechanism. *RSC Adv.* **2016**, *6*, 5223–5232.

(32) Chernorukov, N. G.; Knyazev, A. V.; Bulanov, E. N. Phase transitions and thermal expansion of apatite-structured compounds. *Inorg. Mater.* **2011**, *47*, 172–177.

(33) Oniyama, E.; Wahlbeck, P. G. Application of transpiration theory to TGA data: Calcium carbonate and zinc chloride. *Thermochim. Acta* **1995**, *250*, 41–53.

(34) Ciomartan, D. A.; Clark, R. J. H.; Mcdonald, L. J.; Odlyha, M. Studies on the thermal decomposition of basic lead(II) carbonate by Fourier-transform Raman spectroscopy, X-ray diffraction and thermal analysis. *Dalton Transactions* **1996**, 3639–3645.

(35) Sajadi, S. A. A.; Alamolhoda, A. A. Synthesis and properties of lead oxide carbonate. *Inorg. Mater.* **2006**, *42*, 1099–1103.

(36) Sarig, S.; Kahana, F. Thermal decomposition of basic lead carbonate. *Thermochim. Acta* **1976**, *14*, 263–268.

(37) Ahmad, M.; Ok, Y. S.; Kim, B.-Y.; Ahn, J.-H.; Lee, Y. H.; Zhang, M.; Moon, D. H.; Al-Wabel, M. I.; Lee, S. S. Impact of soybean stover- and pine needle-derived biochars on Pb and As mobility, microbial community, and carbon stability in a contaminated agricultural soil. *J. Environ. Manage.* **2016**, *166*, 131–139.

(38) Jiang, J.; Xu, R. K.; Jiang, T. Y.; Li, Z. Immobilization of Cu(II), Pb(II) and Cd(II) by the addition of rice straw derived biochar to a simulated polluted Ultisol. *J. Hazard. Mater.* **2012**, *229-230*, 145–150.

(39) Ahmad, M.; Lee, S. S.; Lim, J. E.; Lee, S. E.; Cho, J. S.; Moon, D. H.; Hashimoto, Y.; Ok, Y. S. Speciation and phytoavailability of lead and antimony in a small arms range soil amended with mussel shell, cow bone and biochar: EXAFS spectroscopy and chemical extractions. *Chemosphere* **2014**, *95*, 433–441.